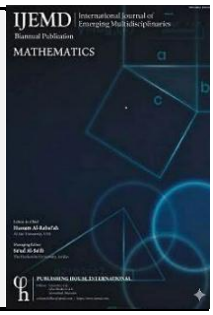
IJEMD-M, 4 (1) (2026) https://doi.org/10.54938/ijemd-m.2026.04.1.857

International Journal of Emerging Multidisciplinaries: Mathematics

Research Paper

Journal Homepage: www.ojs.ijemd.com

ISSN (print): 2790-1998



Thermal Expedition of Viscous Dissipation and Unsteady Slip Flow of Hybrid Nanofluid ($Al_2O_3 - ZnO/H_2O$) Over Inclined Stretching Sheet

Rabia Amjad [1] and Zaffer Elahi [1]*

1. Department of Mathematical Sciences, University of Engineering and Technology, Taxila-Pakistan.

Abstract

The aim of this article is to manipulate the analysis of slip flow and viscous dissipative thermal development of an electrically conducting hybrid nanofluid ($Al_2O_3 - ZnO/H_2O$) over a time-dependent inclined stretching sheet. The principle equations are simplified to a set of nonlinear differential equations by employing variables. The set of equations are solved through built in bvp4c solver on MATLAB. The impacts of pertinent parameters are examined graphically, while tabulated for skin and local Nusselt number specifically on MATLAB. The mixed convection (Richardson number), volume-fraction and viscous dissipation significantly rise the velocity and temperature fields, respectively. The skin-friction grow up with the inclination angle α and magnetic parameter M, while slip H and Prandtl Pr effectively enhance the heat transfer rate as well. The research-outcomes indicate that HNF ($Al_2O_3 - ZnO/H_2O$) is best choice for skin-friction enhancement, while NF (Al_2O_3/H_2O) elevates the heat transfer coefficient prominently. In addition, the effects of HNF on velocity and temperature upsurge for greater values of unsteadiness parameter S. Finally, the study provides greater visibility in optimizing the heat transfer in cooling/heating and advanced thermal management applications.

Keywords: Hybrid nanofluid; Unsteady flow; Inclined sheet; Velocity slip; Boundary layer flow; Heat transfer.

Email Addresses : rabia.amjad@students.uettaxila.edu.pk , zaffer.elahi@uettaxila.edu.pk

1 Introduction

The enhancement of heat-transfer performance has become increasingly important in modern thermal and engineering systems, including heat exchangers, electronic cooling, energy-storage systems, polymer processing, coating technologies, and electromagnetic processing. Conventional fluids such as water, ethylene glycol, and engine oil generally possess relatively low thermal conductivity that resist to transport thermal energy efficiently. The incorporation of nanoparticles into conventional fluids has emerged as an effective technique for improving their thermal characteristics. Such fluids, known as nanofluids, can provide enhanced thermal conductivity and heat-transfer capability owing to the presence of nanosized highly conductive particles. Consequently, nanofluid-based flow and heat-transfer problems have received substantial attention in recent years, particularly for flows induced by moving and stretching surfaces [1,2].

Although mono-nanofluids have demonstrated improved thermal performance, the use of a single nanoparticle may not provide simultaneous optimization of thermal conductivity, viscosity, stability, and other thermophysical characteristics. This limitation motivated the development of hybrid nanofluids, which are produced by dispersing two different types of nanoparticles into a conventional base fluid. The combination of nanoparticles with different thermal and physical properties can provide improved heat-transfer characteristics than conventional fluids and, in many cases, mono-nanofluids. Consequently, hybrid nanofluids have attracted considerable interest for advanced thermal-management applications. Their thermophysical behavior depends on several factors, including nanoparticle type, volume fraction, particle morphology, size, base fluid, and nanoparticle interaction [2,3]. Recent investigations have demonstrated the potential of hybrid nanofluids for improving heat transfer in flow configurations involving stretching surfaces and other technologically important geometries [4,5].

The interaction between an electrically conducting fluid and an externally imposed magnetic field gives rise to magnetohydrodynamic (MHD) flow. When a conducting fluid moves in the presence of a magnetic field, the resulting Lorentz force acts on the fluid and modifies its momentum transport. MHD control is particularly relevant to industrial processes involving electrically conducting fluids, metallurgical operations, electromagnetic pumps, cooling systems, and polymer processing. In nanofluid and hybrid-nanofluid systems, the magnetic field provides an additional mechanism for controlling the hydrodynamic and thermal boundary layers. For example, MHD hybrid-nanofluid flow over stretching surfaces has been shown to exhibit substantial changes in velocity, temperature, skin friction, and heat-transfer rate with variations in the magnetic parameter [4,6].

Stretching-sheet configurations have considerable practical significance because they provide simplified mathematical models for processes such as extrusion, polymer-sheet manufacturing, continuous casting, glass-fiber production, metal coating, and plastic-film drawing. Particularly, the consideration of an inclined stretching sheet

introduces the effect of gravitational acceleration along the surface. The inclination angle therefore influences the buoyancy force and consequently modifies the momentum and thermal boundary layers. Alabdulhadi *et al*. [7] investigated hybrid-nanofluid flow over an inclined surface in the presence of magnetic-field demonstrated that surface inclination provides an important mechanism for controlling the flow and heat-transfer characteristics. More recently, inclined MHD hybrid-nanofluid configurations have also been investigated with additional thermal and slip effects [8].

Another important physical feature in boundary-layer flows is the interaction between the fluid and the solid surface, is known as slip condition. A finite relative velocity exists between the fluid and the stretching surface because of velocity-slip condition. The resulting modification of the wall velocity gradient directly affects the skin-friction coefficient and can also influence the thermal boundary layer and heat-transfer rate. Studies on MHD nanofluid flow with velocity-slip conditions have shown that increasing the slip parameter can significantly modify the velocity profile, wall shear stress, and Nusselt number [9]. Moreover, Navier-slip effects have been incorporated into MHD hybrid-nanofluid flow over porous stretching/shrinking sheets, emphasizing the importance of wall slip in controlling transport phenomena [10]. Hybrid-nanofluid flow with velocity and thermal slip conditions has been investigated in different stretching-sheet configurations [11,12].

A brief survey of hybrid nanofluid has been presented in different geometries below. Khan *et al*. [13] investigated MHD hybrid nanofluid flow over an exponentially stretching sheet with slip conditions and reported that variations in the magnetic parameter significantly affect the velocity and heat-transfer characteristics. Jawad *et al*. [14] demonstrated that increasing the magnetic parameter decreases the velocity distribution while influencing the heat-transfer rate in an hybrid nanofluid ($Al_2O_3 - Cu$) over a stretching (or shrinking) sheet. Al-Zubaidi *et al.* [15] analyzed the slip flow of MHD nanofluid past over a sheet using Keller box simulation. Suresh *et al*. [16] prepared hybrid ($Al_2O_3 - Cu/H_2O$) suspension by a two-step method and characterized its thermophysical properties. Toghraie *et al*. [17] measured the thermal conductivity of a ($ZnO - Ti_2O$) mixture while, Hayat and Nadeem [18] reported a comparable advantage for hybrid nanofluid ($Ag - CuO/H_2O$). Usman *et al*. [19] examined hybrid nanofluid ($Cu - Al_2O_3/H_2O$) through a permeable surface with nonlinear radiation and variable thermal conductivity. Anuar *et al.* [20] investigated hybrid nanofluid ($Ag - MgO/H_2O$) over an inclined permeable stretching and shrinking sheet under a buoyancy force. Wahid *et al.* [21] demonstrated that velocity slip lowers skin friction while modify the local Nusselt number.

Although the factors like velocity-slip, hybrid nanoparticles, heat transport and MHD flow, thermal conductivity, and heat generation/absorption are discussed explicitly in stretching surfaces, sheets, plate geometries in steady environment, but limited literature with hybrid nanofluid in unsteady case is available over inclined stretching sheet.

So, further investigation is required to understand the coupled effects of surface inclination, magnetic field, hybrid nanoparticles, and velocity slip in stretching-sheet flows.

Motivated by the aforementioned considerations, the present study focuses on **"Thermal expedition of viscous dissipation and unsteady slip flow of hybrid nanofluid ($Al_2O_3 - ZnO/H_2O$) over inclined stretching sheet"**. The mathematical model incorporates the effects of hybrid nanoparticles, magnetic field, gravitational force associated with the inclination of the sheet, and velocity slip at the stretching surface. Appropriate similarity transformations are employed to reduce the governing boundary-layer equations to a system of nonlinear ordinary differential equations, which is solved numerically. The effects of the governing parameters on the velocity, temperature, skin-friction coefficient, and local Nusselt number are examined in detail. Particular attention is given to the comparative thermal performance of the hybrid nanofluid and the corresponding base/mono-nanofluid system. The results are expected to provide useful theoretical insight into the control of MHD hybrid-nanofluid flow and heat transfer over inclined stretching surfaces and may be relevant to advanced cooling, coating, polymer-processing, and thermal-management applications.

The organization of the article is, as follows mathematical description of the proposed model is presented in Section 2, while the solution methodology and numerical technique bvp4c is described in Section 3. Section 4 presents the detailed graphical discussion of the scrutinized results as well as numerical computation of skin and Nusselt number. The research-outcomes are summarized in conclusion Section 5.

Nomenclature

u, v	Velocity components	α	Inclination angle
a, b	Dimensional constants	β	Thermal expansion coefficient
T	Fluid temperature	c_p	Specific heat
T_∞	Ambient temperature	λ	Mixed convection parameter
T_s	Surface Temperature	σ	Electric conductivity
Re	Reynolds number	**Subscripts**	
Pr	Prandtl number	f	Base fluid
Ec	Eckert number	nf	Nanofluid
M	Magnetic parameter	hnf	Hybrid nanofluid
H	Slip parameter	1	Al_2O_3 solid volume fraction
S	Unsteady parameter	2	ZnO solid volume fraction
Bi	Biot number		

		Abbreviations	
Gr	Grashof number	NF	Nanofluid
g	Gravity	HNF	Hybrid Nanofluid
C_f	Skin coefficient	NP	Nanoparticle
Nu	Nusselt number		
Greek Symbols			
ν	Kinematic viscosity		
ρ	Fluid density		
μ	Dynamic viscosity		
κ	Thermal conductivity		
ψ	Stream function		
ϕ_1	Al_2O_3 – NP		
ϕ_2	ZnO – NP		

2 Problem Formulation

A two-dimensional boundary layer slip flow of an electrically conducting hybrid nanofluid ($Al_2O_3 - \mathrm{ZnO}/\mathrm{H_2O}$) over a stretching sheet inclined at an angle α is considered. The sheet is stretched continuously along x-axis with velocity $U_s(x) = \frac{ax}{1-bt}$, while applied magnetic field $B(t) = \frac{B_0}{\sqrt{1-bt}}$ is taking along y-axis perpendicular to the moving fluid (see Fig. 1).

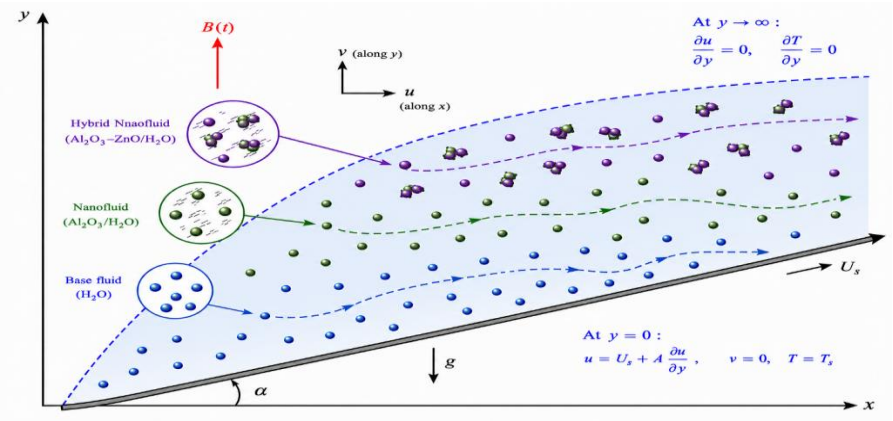


Figure 1: Flow Geometry

Suppose that the velocity components of fluid are $u(x, y, t)$ and $v(x, y, t)$ taken along the coordinates axes in the rectangular coordinate system with temperature $T(x, y, t)$ of the fluid. T_s and T_∞ be the surface and ambient temperatures of the fluid such that $T_s > T_\infty$ and that $T_s = T_\infty + \frac{T_0\, x}{(1-bt)^2}$. Further, viscous dissipation is also

incorporated in the model to analyze the enhancement of heat transfer in the energy equation.

Underlying these assumptions stated above, the boundary layer flow equations of hybrid nanofluid model are explained below, as (Afridi *et al*. [7])

$$\frac{\partial u}{\partial x}+\frac{\partial v}{\partial y}=0, \tag{1}$$

$$\frac{\partial u}{\partial t}+u\frac{\partial u}{\partial x}+v\frac{\partial u}{\partial y}=\frac{\mu_{hnf}}{\rho_{hnf}}\frac{\partial^2 u}{\partial y^2}+\frac{(\rho\beta)_{hnf}}{\rho_{hnf}}g(T-T_\infty)cos\alpha-\frac{\sigma_{hnf}}{\rho_{hnf}}\,\mathrm{B}^2(t)\,u, \tag{2}$$

$$\frac{\partial T}{\partial t}+u\frac{\partial T}{\partial x}+v\frac{\partial T}{\partial y}=\frac{k_{hnf}}{(\rho c_p)_{hnf}}\frac{\partial^2 T}{\partial y^2}+\frac{\mu_{hnf}}{(\rho c_p)_{hnf}}\left(\frac{\partial u}{\partial y}\right)^2. \tag{3}$$

The relevant boundary conditions are (Hayat *et al.* [22])

$$\left.\begin{aligned} u=U_s+Av_f\frac{\partial u}{\partial y},\ v=0,\ T=T_s, \quad & y=0,\\ \frac{\partial u}{\partial y}=0,\ \ \frac{\partial T}{\partial y}=0, \quad & y\to\infty. \end{aligned}\right\} \tag{4}$$

The correlation of a general hybrid nanofluid are defined, as (Devi and Devi [23])

$$a_1=\frac{\mu_{hnf}}{\mu_f}=(1-(\phi_1+\phi_2)+\phi_1\phi_2)^{-\frac{5}{2}}, a_2=\frac{\sigma_{hnf}}{\sigma_f}=\frac{\sigma_2+2\sigma_{bf}-2\phi_2(\sigma_{bf}-\sigma_2)}{\sigma_2+2\sigma_{bf}+\sigma_2(\sigma_{bf}-\sigma_2)}*\frac{\sigma_1+2\sigma_f-2\phi_1(\sigma_f-\sigma_1)}{\sigma_1+2\sigma_f+\varphi_1(\sigma_f-\sigma_1)},$$

$$a_3=\frac{(\rho\beta)_{hnf}}{(\rho\beta)_f}=(1-\phi_2)\left[(1-\phi_1)+\phi_1\frac{(\rho\beta)_1}{(\rho\beta)_f}\right]+\phi_2\frac{(\rho\beta)_2}{(\rho\beta)_f},$$

$$a_4=\frac{\rho_{hnf}}{\rho_f}=(1-\phi_2)\left[(1-\phi_1)+\phi_1\left(\frac{\rho_1}{\rho_f}\right)\right]+\phi_2\left(\frac{\rho_2}{\rho_f}\right),$$

$$b_1=\frac{k_{hnf}}{k_f}=\frac{k_2+2k_{bf}-2\phi_2(k_{bf}-k_2)}{k_2+2k_{bf}+\phi_2(k_{bf}-k_2)}*\frac{k_1+2k_f-2\phi_1(k_f-k_1)}{k_1+2k_f+\phi_1(k_f-k_1)},$$

$$b_2=\frac{(\rho c_p)_{hnf}}{(\rho c_p)_f}=(1-\phi_2)\left[(1-\phi_1)+\phi_1\frac{(\rho c_p)_1}{(\rho c_p)_f}\right]+\phi_2\frac{(\rho c_p)_2}{(\rho c_p)_f},$$

where $\phi_1=\phi_2=0$ signify the regular fluid.

The article uses the following thermophysical characteristics of Aluminium Oxide (Al_2O_3), Zinc Oxide (ZnO), and base fluid water (H_2O) are provided in Table 1.

Table 1: Thermophysical characteristics of (Al_2O_3-ZnO/H_2O) [24-25]

Properties	Al_2O_3	ZnO	H_2O
$\rho(kgm^{-3})$	3970	5600	997.1
$c_\rho(JKg^{-1}K^{-1})$	765	495	4179
$\kappa(Wm^{-1}k^{-1})$	40	13	0.613
$\beta(k^{-1})$	0.85×10^{-5}	5.0×10^{-6}	21×10^{-5}
$\sigma(s/m)$	3.69×10^{7}	7.261×10^{-5}	5.5×10^{-4}

Following transformations (Hayat *et al*. [22]) are employed to the governing model to make it dimensionless, given below

$$\eta = \sqrt{\frac{a}{v_f(1-bt)}}\, y, \qquad \theta(\eta) = \frac{T - T_\infty}{T_s - T_\infty}, \qquad \psi = \sqrt{\frac{av_f}{1-bt}}\, x f(\eta). \tag{5}$$

The flow function ψ characterizes the velocity, as $u = \frac{ax}{1-bt}\, f'(\eta)$ and $v = -\sqrt{\frac{av_f}{1-bt}} f(\eta)$ that satisfy Eqn. (1) directly. The principle Eqns. (2-3) together with (4) can be rewritten, as

$$R_1 f''' - f'^2 + ff'' - R_3 M f' - \mathrm{S}\left(f' + \frac{\eta}{2} f''\right) + \mathrm{R}_4 \lambda\theta cos\alpha = 0, \tag{6}$$

$$\frac{R_2}{Pr}\,\theta'' + f'\theta - f\theta' - S\left(2\theta - \frac{\eta}{2}\theta'\right) + \mathrm{R}_5 \mathrm{Ec}\, f''^2 = 0, \tag{7}$$

and

$$f(0) = 0, f'(0) = 1 + Hf"(0),\ \theta(0) = 1, f'(\infty) = 0, \theta(\infty) = 0, \tag{8}$$

$\lambda = \frac{Gr}{Re_x^2}$, $Gr = \frac{\mathrm{g}\beta_f(T_s - T_\infty)x^3}{v_f^2}$, $Re_x = \frac{xU_s}{v_f}$, $M = \frac{\sigma_f B_0^2}{a\rho_f}$, $Pr = \frac{v_f}{\alpha_f}$, $S = \frac{b}{a}$, $Ec = \frac{U_s^2}{(T_s - T_\infty)(c_p)_f}$, and

$H = A\sqrt{\frac{v_f U_s}{x}}$ are the physical parameters appeared in Eqns. (6-8). Moreover, $R_1 = \frac{a_1}{a_4}, R_2 = \frac{b_1}{b_2}$, $R_3 = \frac{a_2}{a_4}, R_4 = \frac{a_3}{a_4}, R_5 = \frac{a_1}{b_2}$ represent constants, as in [26].

Physical Quantities

Nusselt number (Nu_x) and the skin coefficient (C_f) are critical engineering parameters govern momentum and heat transport at the fluid-solid interface. Skin quantifies the shear stress and drag exerted by the fluid, while the Nusselt number measures the efficiency of convective heat transfer at the surface are obtained as

$$C_f = \frac{\mu_{hnf}}{\rho_f U_s^2}\left(\frac{\partial u}{\partial y}\right)_{y=0} \text{ and } Nu_x = -\left(\frac{k_{hnf}}{k_f}\right)\frac{x}{T_s - T_\infty}\left(\frac{\partial T}{\partial y}\right)_{y=0}. \tag{9}$$

Thus, non-dimensional components C_f and $\mathrm{N}u_x$ are delineated, as

$$Re_x^{1/2} C_f = a_1 f''(0) \text{ and } Re^{-1/2} Nu_x = -b_1\, \theta'(0) \tag{10}$$

3 Solution Methodology

The system of highly nonlinear ordinary differential equations governing the boundary value problem derived from the flow and heat transfer analysis of hybrid nanofluid over an inclined stretching sheet under slip and viscous dissipation effect, solved numerically using bvp4c solver. This solver, originally developed by Shampine *et al*. [27], implements a collocation technique that making it particularly well-suited for handling stiff and nonlinear boundary value problems of the type addressed in Eqns. (6-7). The step-by-step numerical procedure adopted to obtain

accurate and convergent solutions is systematically outlined below.

Consider the new variables

$$y_1 = f,\ y_1' = y_2,\ y_2' = y_3,\ y_3' = yy_1,\ y_4 = \theta\ , y_4' = y_5,\ y_5' = yy_2. \tag{11}$$

The following system first order equations is obtained, as follows

$$y_1' = y_2, y_2' = y_3, yy_1 = \frac{1}{R_1}\left[y_2^2 - y_1 y_3 + R_3 M y_2 + S\left(y_2 + \frac{\eta}{2} y_3\right) - R_4\,\lambda\,\theta\,cos\alpha\right], y_4' = y_5,$$

$$yy_2 = \frac{Pr}{R_2}\left[y_2 y_4 - y_1 y_5 + S\left(2y_4 + \frac{\eta}{2} y_5\right) - R_5 Ec\, y_3^2\right]. \tag{12}$$

The associated constraints (8) with variables defined in (11) are

$$y_1(0) = 0, y_2(0) = 1 + H y_3(0), y_4(0) = 1, y_3(\infty) = 0, y_5(\infty) = 0. \tag{13}$$

Since the system (12) contain five unknowns, therefore five initial conditions are required to get the solution. But only three initial conditions exist in (13). So, choosing the initial guesses for $y_3(0)$ and $y_5(0)$ in such a way that the result will converge if the error of $y_3(\infty)$ and $y_5(\infty)$ is lesser than the tolerance 10^{-8}, otherwise the initial guesses moderate till the desired accuracy achieved. The value of boundary layer η_∞ for this problem is chosen 10 satisfying $y_3(\infty) \to 0$ and $y_5(\infty) \to 0$. The accuracy of the scheme is tested by comparing results with published work presented in the following Table 2.

Validation of Result

The scrutinized results of Nusselt number for ($\phi_1 = \phi_2 = 0$) are compared with Anuar *et al*. [20] and Rosca and Pop [28] across different values of λ taking $S = M = \alpha = 0$, and $Pr = 1$. Table 2 reflects the excellent agreement of the results that reveal the accuracy and reliability of the scheme bvp4c, establishing strong confidence in the developed algorithm for the hybrid nanofluid model.

Table 2: Comparison of Nusselt Number

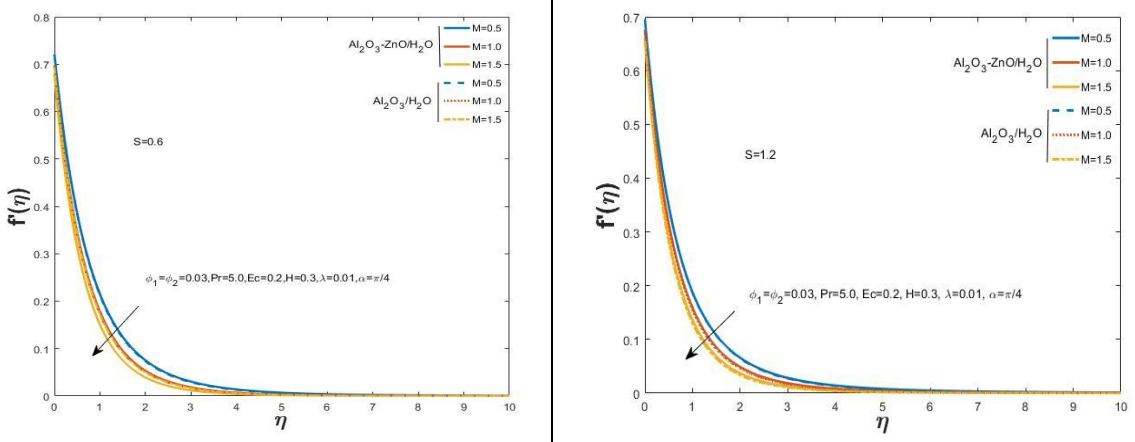
λ	Anuar *et al*. [20]	Rosca and Pop [28]	BVP4C Results
0	1.000008	1.0000	1.000008
1	1.087275	1.0872	1.087275
10	1.371564	1.3715	1.371564

4 Results and discussion

In this Section, graphical results of fluid velocity and temperature across various primary parameters are developed on MATLAB and showed in Figures 1-10, while results of skin and Nusselt number are presented in Tables 3-4. All necessary computations are done on MATLAB, taking $\varphi_1 = \varphi_2 = 0.03$, $\mathrm{M} = 1.0, \mathrm{Pr} = 5.0, \mathrm{Ec} = 0.2, \mathrm{H} = 0.3, \lambda = 0.01$, and $\alpha = \frac{\pi}{4}$ as default parameters.

4.1 Velocity Graphs

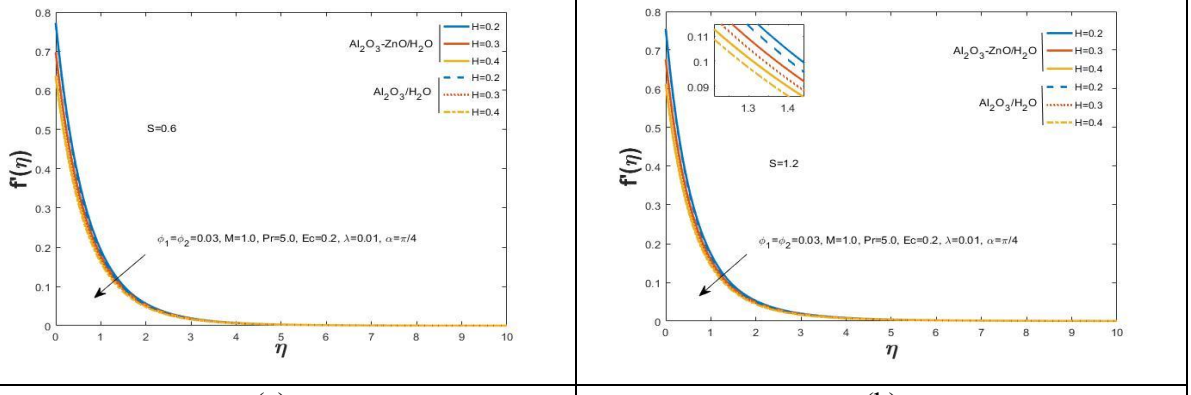
Fig.(2) shows the magnetic impact on horizontal velocity for both HNF $(Al_2O_3 - ZnO/H_2O)$ and NF (Al_2O_3/H_2O). The velocity profiles of HNF and NF decreases as M increases for $S = 0.6$ and $S = 1.2$, shown in Fig.2(a) and Fig.2(b). Since leading fluid forms a Lorentz force when it comes into contact of magnetic fluid, therefore it works against fluid velocity by producing damping effect. So, it is getting slow down the fluid motion due to which velocity profile drops.



(a) (b)

Figure 2: Effects of $f'(\eta)$ at M

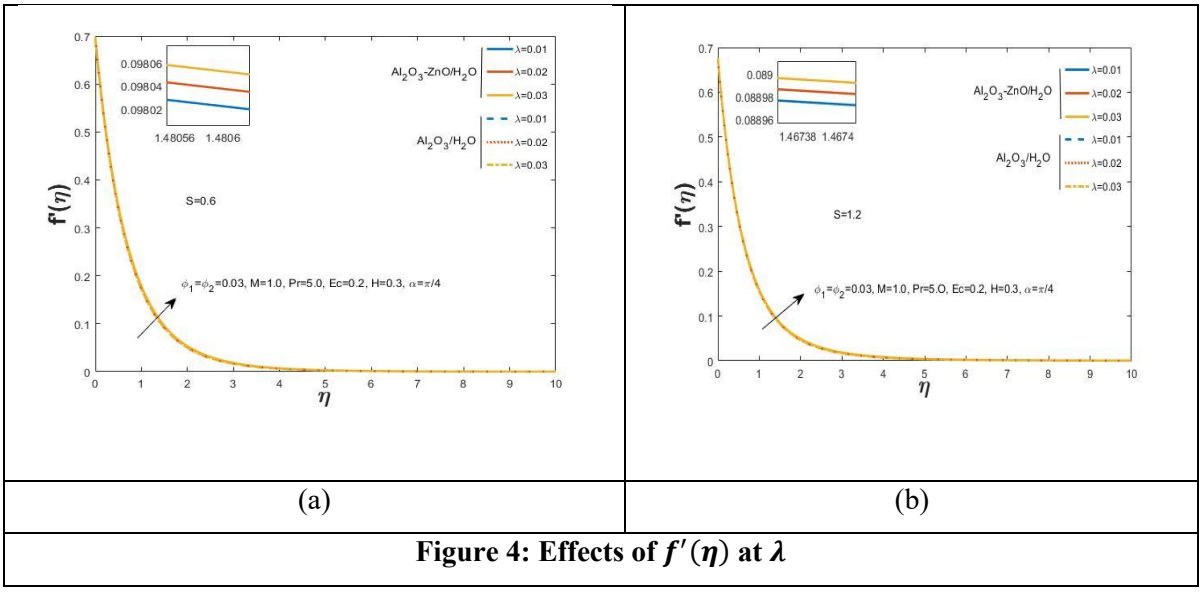
In Fig.3(a) and Fig.3(b), similar decreasing trend is noted for HNF and NF as slip parameter H increases. Fluid does not move at the same speed closer to the sheet in the presence of slip, the fluid velocity drops. It should also be noted that HNF $(Al_2O_3 - ZnO/H_2O)$ significantly effect on $f'(\eta)$ than NF (Al_2O_3/H_2O).



(a) (b)

Figure 3: Effects of $f'(\eta)$ at H

The influence of mixed convection parameter on $f'(\eta)$ is plotted in Fig.4, where λ set a raising trend of velocity of both types of HNF $(Al_2O_3 - ZnO/H_2O)$ and NF (Al_2O_3/H_2O) as shown in Fig.4(a) and Fig.4(b). Buoyancy forces dominantly lift up the movement of fluid particles in the flow domain as λ grows, leads to rise in velocity profile.

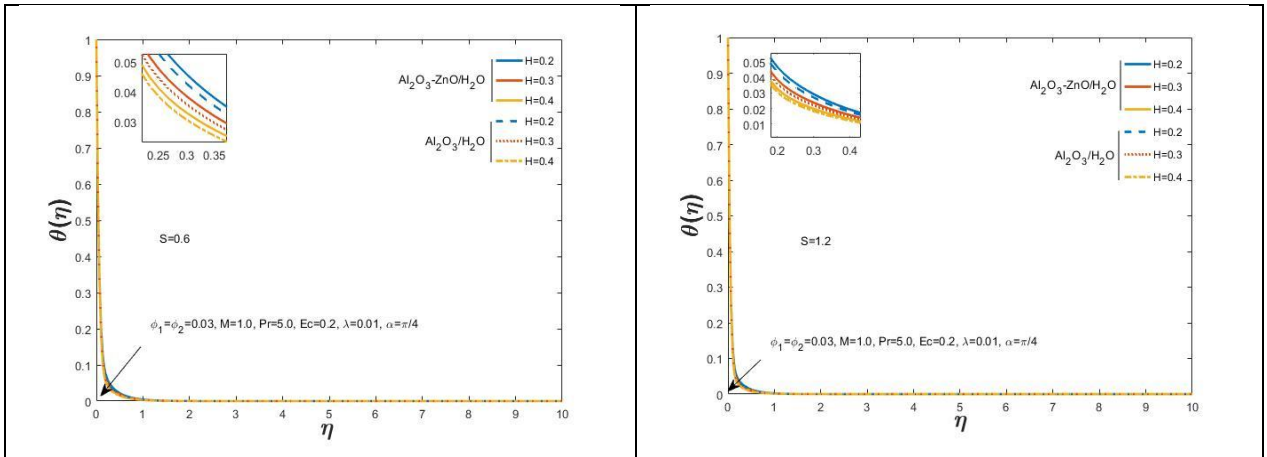


(a) (b)

Figure 4: Effects of $f'(\eta)$ at λ

4.2 Temperature Graphs

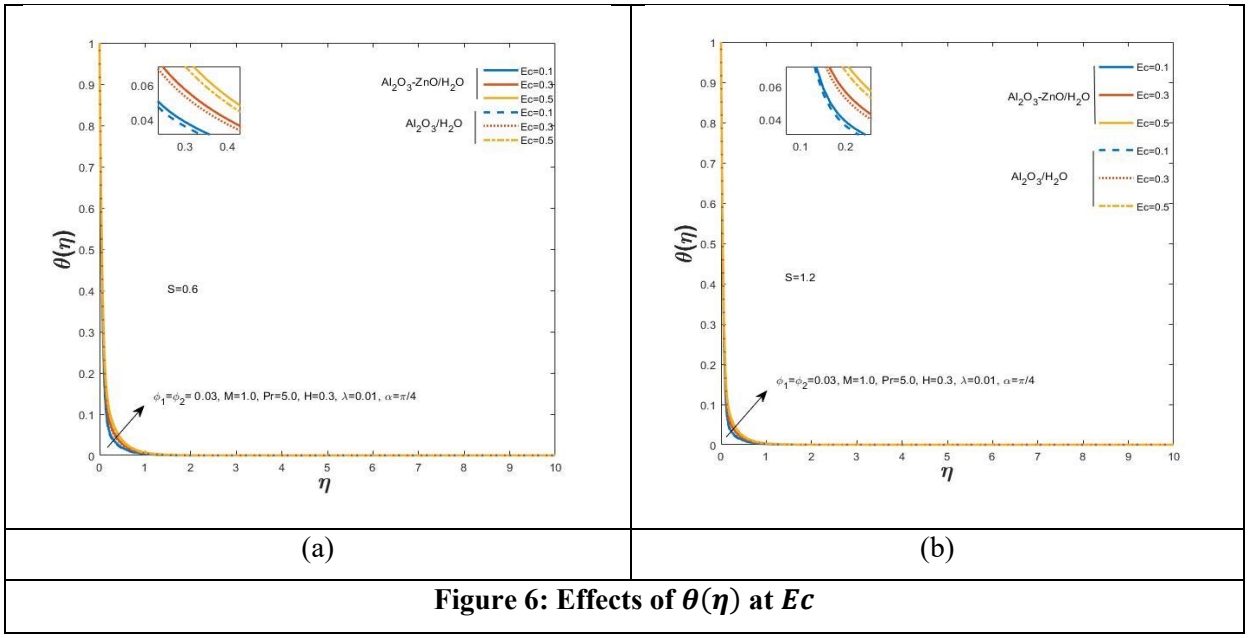
The impact of slip H on temperature $\theta(\eta)$ for HNF $(Al_2O_3 - ZnO/H_2O)$ and NF (Al_2O_3/H_2O) is illustrated in Fig.5 (a) when $S = 0.6$ and $S = 1.2$. Both Figs.5(a) and 5(b) reveal that increasing H decreases temperature $\theta(\eta)$ near the wall, as reduced frictional interaction lowers viscous heating. It is worth mentioning that HNF dominantly effect the temperature as compared to NF.



(a) (b)

Figure 5: Effects of $\theta(\eta)$ at H

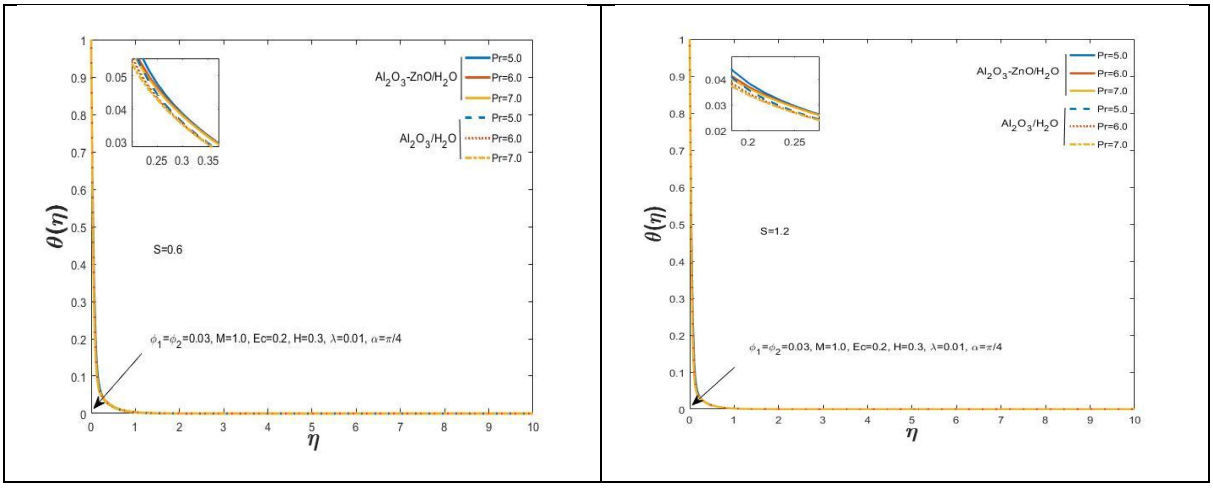
Viscous dissipation (or Eckert number) effect for both HNF and NF on temperature is drawn in Fig.6 when $S = 0.6$ and $S = 1.2$. It is clearly shown in Fig.6(a) and Fig.6(b) that HNF $(Al_2O_3 - ZnO/H_2O)$ and NF (Al_2O_3/H_2O) boost up temperature in both cases as Ec increases. Physically viscous dissipation (Ec) acts as a heat source in the energy equation, converting kinetic energy into thermal energy near the boundary layer.



(a) (b)

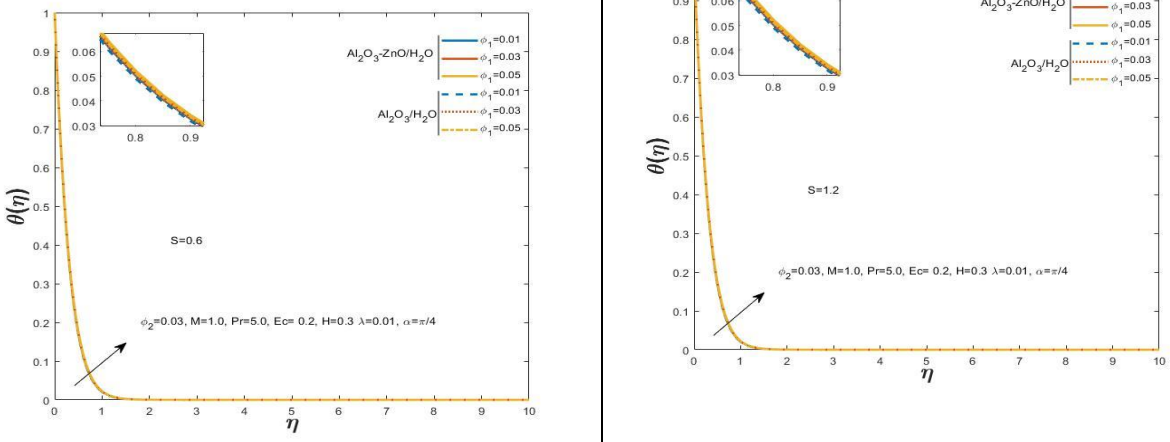
Figure 6: Effects of $\theta(\eta)$ at Ec

Fig.7(a) and Fig.7(b) demonstrate how Prandtl (Pr) influence on temperature $\theta(\eta)$ for both hybrid and mono nanofluids for $S = 0.6$ and $S = 1.2$. Higher Pr are directly connected to decreasing the thermal diffusivity, which plays an important role in reducing the capability of heat to transfer inside the fluid. As a result, the overall fluid temperature drops. Moreover, this decrease in temperature is more rapid in the case of the NF as compared to that of the HNF.



(a)	(b)
Figure 7: Effects of $\theta(\eta)$ at Pr	

The impact of volume-fraction (ϕ_1) on temperature is depicted in Fig.8(a) and Fig.8(b) for $S = 0.6$ and $S = 1.2$. It is evident from these graphs that both fluids HNF and NF experience higher temperature as ϕ_1 increases. However, this temperature rise is more apparent in the case of HNF, implying that the combined effects of Al_2O_3 and ZnO nanoparticles give it greater thermal conductivity.



(a)	(b)
Figure 8: Effects of $\theta(\eta)$ at ϕ_1	

4.3 Engineering Applications

The analysis of time-dependent skin-friction is recorded for both HNF $(Al_2O_3 - ZnO/H_2O)$ and NF (Al_2O_3/H_2O) across different parameters values in Table 3. HNF $(Al_2O_3 - ZnO/H_2O)$ significantly rise the skin-friction relative to NF (Al_2O_3/H_2O) for increasing values of M and α, while opposite behavior is noted for λ and H.

Table 3: Results of skin-friction

S	λ	M	H	α	HNF Results	NF Results
	0.01	1.0	0.3	$\pi/4$	1.1734994	1.1011618
	0.02				1.1732158	1.1008777
	0.03				1.1729321	1.1005935
	0.01	**0.5**			1.0832164	0.9295586
		1.0			1.1728902	1.0160661
		1.5			1.2496288	1.0887885
0.6			**0.2**		1.3236773	1.2426800
			0.3		1.1732994	1.1011618
			0.4		1.0557773	0.9902396
				$\boldsymbol{\pi/6}$	1.1734357	1.1010980
				$\boldsymbol{\pi/4}$	1.1734994	1.1011618
				$\boldsymbol{\pi/3}$	1.1735825	1.1012451
	0.01				1.2566940	1.1735188
	0.02				1.2564786	1.1733024
	0.03				1.2562632	1.1730859
	0.01	**0.5**			1.1807498	1.0831717
		1.0			1.3224026	1.1465591
		1.5			1.3228802	1.2421568
1.2			**0.2**		1.4255485	1.3315578
			0.3		1.1256694	1.1735188
			0.4		1.1254017	1.0506208
				$\boldsymbol{\pi/6}$	1.2566456	1.1734701
				$\boldsymbol{\pi/4}$	1.2566694	1.1735188
				$\boldsymbol{\pi/3}$	1.2567571	1.1735822

Moreover, Table 4 reflects rate of heat transport effect across diverse parameter values. The heat transport coefficient is increased for H and Pr significantly affected by NF (Al_2O_3/H_2O), but declining effects are found at α, M and Ec.

Table 4: Results of Nusselt number

S	M	Pr	Ec	H	α	HNF Results	NF Results
0.6	**0.5**	5.0	0.2	0.3	$\pi/4$	0.6324856	0.6400121
	1.0					0.6174757	0.6238055
	1.5					0.6042509	0.6097584
	1.0	**5.0**				0.6174757	0.6238055
		6.0				0.6756480	0.6826558
		7.0				0.7290969	0.9464135
			0.1			0.6520807	0.6564984
			0.3			0.5828748	0.5911165
			0.5			0.5136851	0.5257501
				0.2		0.6159906	0.6234798
				0.3		0.6174757	0.6238055
				0.4		0.6168105	0.6222924
					$\boldsymbol{\pi/6}$	0.6174821	0.6238122
					$\boldsymbol{\pi/4}$	0.6174757	0.6238055
					$\boldsymbol{\pi/3}$	0.6174673	0.6237968
1.2	**0.5**					0.8036438	0.8122963
	1.0					0.7931928	0.8009483
	1.5					0.7838067	0.7909104
	1.0	**5.0**				0.7931928	0.8009483
		6.0				0.8681770	0.8767443
		7.0				0.9370980	0.9464135
			0.1			0.8244449	0.8302201
			0.3			0.7619410	0.7716768
			0.5			0.6994442	0.7131401
				0.2		0.7896095	0.7985710
				0.3		0.7931926	0.8009483
				0.4		0.7942453	0.8011488
					$\boldsymbol{\pi/6}$	0.7931965	0.8009522
					$\boldsymbol{\pi/4}$	0.7931928	0.8009483
					$\boldsymbol{\pi/3}$	0.7931878	0.8009431

5 Conclusion

The study focuses on heat transport development analysis of hybrid nanofluid ($Al_2O_3 - ZnO/H_2O$) over an unsteady inclined stretching sheet under slip and viscous dissipation effect. Similarity solutions of converted equations by means of bvp4c solver. Following conclusions are drawn from the study.

- Higher values of Richardson number (λ) elevate the velocity field with HNF and NF.
- Slip and magnetic parameters suppress the horizontal velocity profile.
- Higher Prandtl and slip both decelerate the thermal profile.
- Viscous dissipation (Ec) and volume-fraction (ϕ_1) significantly grow up the thermal profile.
- Both parameters M and α with HNF ($Al_2O_3 - ZnO/H_2O$) effectively rise the skin-friction, while the reverse trend is seen in the case of heat transfer rate.
- Increasing H and λ decay the velocity gradient gradually.
- Nusselt number diminishes as H increases for $S = 0.6$, but it alters when $S = 1.2$ and this effect is strongly appeared with NF (Al_2O_3/H_2O).
- Pr dominantly accelerate the Nusselt number in the presence of NF (Al_2O_3/H_2O), but opposite in Ec.

References

[1] J. Buongiorno, *Convective transport in nanofluids*, Journal of Heat Transfer, 128 (2006), 240–250.

[2] S. U. S. Choi, *Enhancing thermal conductivity of fluids with nanoparticles*, ASME International Mechanical Engineering Congress and Exposition, 17421 (1995) 99-105.

[3] J. Sarkar, P. Ghosh, and A. Adil, *A review on hybrid nanofluids*: *Recent research, development and applications*, Renewable and Sustainable Energy Reviews, 43 (2015), 164–177.

[4] E. H. Aly and I. Pop, *MHD flow and heat transfer near stagnation point over a stretching/shrinking surface with partial slip and viscous dissipation: Hybrid nanofluid versus nanofluid*, Powder Technology, 367 (2020), 192–205.

[5] T. S. Kumar, *Hybrid nanofluid slip flow and heat transfer over a stretching surface*, Partial Differential Equations in Applied Mathematics, 4 (2021) 100070.

[6] A. S. Khan, H.-Y. Xu, and W. Khan, *Magnetohydrodynamic hybrid nanofluid flow past an exponentially stretching sheet with slip conditions*, Mathematics, 9 (2021) 3291.

[7] M. I. Afridi, M. Qasim, I. Khan, S. Shafie, and A. S. Alshomrani, *Entropy generation in magneto-hydrodynamic mixed convection flow over an inclined stretching sheet*, Entropy, 19 (1) (2016) 10.

[8] S. M. Sachhin, U. S. Mahabaleshwar, H. N. Huang, B. Sunden, and D. Zeidan, *An influence of temperature jump and Navier's slip-on hybrid nanofluid flow over a permeable stretching/shrinking sheet with heat transfer and inclined MHD*, Nanotechnology, 35 (11) (2023) 115401.

[9] D. Ramya, R. S. Raju, J.A. Rao, and A. J. Chamka, *Effects of velocity and thermal wall slip on magnetohydrodynamics (MHD) boundary-layer viscous flow and heat transfer of a nanofluid over a non-linearly stretching sheet*, Propulsion and Power Research, 7 (2018) 182–195.

[10] T. Maranna, G. M. Sachin, U. S. Mahabaleshwar, L. M. Pérez, and I. V. Shevchuk, *Impact of Navier's slip and MHD on a hybrid nanofluid flow over a porous stretching/shrinking sheet with heat transfer*, Fluids, 9 (8) (2024) 180.

[11] S. Sharma, and S. Jain, *Convective heat transfer flow of MHD hybrid nanofluid over a stretching sheet with velocity and thermal slip*, International Journal of Mathematics and Physics, 15 (2024) 58 – 74.

[12] M. Ramzan, A. Dawar, A. Saeed, P. Kumam, W. Watthayu, and W. Kumam, *Heat transfer analysis of the mixed convective flow of magnetohydrodynamic hybrid nanofluid past a stretching sheet with velocity and thermal slip conditions*. PLoS One, 16 (12) (2021) e0260854.

[13] W. A. Khan and I. Pop, *Boundary-layer flow of a nanofluid past a stretching sheet,* International Journal of heat and mass Transfer, 53 (11-12) (2010) 2477-2483.

[14] M Jawad, A Saeed, A Tassaddiq, A Khan, T Gul, P Kumam, and Z Shah, *Insight into the dynamics of second grade hybrid radiative nanofluid flow within the boundary layer subject to Lorentz force,* Scientific Reports, 11 (1) (2021) 4894.

[15] A. Al-Zubaidi, H. Abutuqayqah, B. Ahmad, S. Bibi, T. Abbas, and S. Saleem, *Analysis of slip condition in MHD nanofluid flow over stretching sheet in presence of viscous dissipation: Keller box simulations,* Alexandria Engineering Journal, 82 (2023) 26-34.

[16] S. Suresh, K. P. Venkitaraj, P. Selvakumar, and M. Chandrasekar, *Synthesis of $Al_2O_3 - Cu$/water hybrid nanofluids using two step method and its thermo physical* properties, Colloids and Surfaces A: Physicochemical and Engineering Aspects, 388 (1-3) (2011) 41-48.

[17] D. Toghraie, V. A. Chaharsoghi, and M. Afrand, *Measurement of thermal conductivity of $ZnO - TiO_2/EG$ hybrid nanofluid: Effects of temperature and nanoparticles concentration*, Journal of Thermal Analysis and Calorimetry, 125 (1) (2016) 527-535.

[18] T. Hayat and S. Nadeem, *Heat transfer enhancement with $Ag - CuO$/water hybrid nanofluid,* Results in Physics, 7 (2017) 2317-2324.

[19] M. Usman, M. Hamid, T. Zubair, R. U. Haq, and W. Wang, *$Cu - Al_2O_3$/Water hybrid nanofluid through a permeable surface in the presence of nonlinear radiation and variable thermal conductivity via LSM,* International Journal of Heat and Mass Transfer, 126 (2018) 1347-1356.

[20] N. S. Anuar, N. Bachok, and I. Pop, *Influence of buoyancy force on $Ag - MgO$/water hybrid nanofluid flow in an inclined permeable stretching/shrinking sheet,* International Communications in Heat and Mass Transfer, 123 (2021) 105236.

[21] N. S. Wahid, N. M. Arifin, N. S. Khashi'ie, and I. Pop, *Hybrid nanofluid slip flow over an exponentially*

stretching/shrinking permeable sheet with heat generation, Mathematics, 9 (1) (2020) 30.

[22] U. Hayat, R. Ali, S. Shaiq, and A. Shahzad, *A numerical study on thin film flow and heat transfer enhancement for copper nanoparticles dispersed in ethylene glycol*, Reviews on Advanced Materials Science, 62 (1) (2023) 20220320.

[23] S. U. S. Devi and S. P. A. Devi, *Numerical investigation of three-dimensional hybrid* $Cu\text{-}Al_2O_3$ */water nanofluid flow over a stretching sheet with effecting Lorentz force subject to Newtonian heating, Canadian Journal of Physics,* 94 (5) (2016) 490-496.

[24] T Singla, M Verma, B Kumar, S Sharma, *Analysis of stagnation flow characteristics in hybrid nanofluid impingement: velocity slip, convective heat transfer and varied inclination angles,* Arabian Journal for Science and Engineering, 49 (7) (2024) 10121-10136.

[25] G. Yalçın, S. Öztuna, A. S. Dalkılıç, and S. Wongwises, *Measurement of thermal conductivity and viscosity of* $ZnO\text{-}SiO_2$ *hybrid nanofluids, J*ournal of Thermal Analysis and Calorimetry, 147 (15) (2022) 8243-8259.

[26] S. A. Qureshi, A. Shahzad, and S. Shaiq, *Numerical treatment of the magnetised dissipative thin-film hybrid nanofluid* $(SWCNT\text{-}MWCTN/H_2O)$ *flow and heat transfer over an unsteady stretching sheet with partial slip and convective boundary conditions,* International Journal of Ambient Energy, 47 (1) (2026) 2660869.

[27] L. F. Shampine, I Gladwell, S Thompson, and I Gladwell, *Solving ODEs with matlab*, Cambridge University Press, Cambridge, 70, 2003.

[28] A. V. Roşca and I. Pop, *Flow and heat transfer over a vertical permeable stretching/shrinking sheet with a second order slip,* International Journal of heat and mass Transfer, 60 (2013) 355-364.